# Coupled-channels study of the $\pi^- p \to \eta n$ process

J. Durand,[1] B. Juliá-Díaz,[2,3] T.-S. H. Lee,[3,4] B. Saghai,[1] and T. Sato[3,5]

[1]*Institut de Recherche sur les lois Fondamentales de l'Univers, DSM/IRFU, CEA/Saclay, F-91191 Gif-sur-Yvette, France*

[2]*Departament d'Estructura i Constituents de la Matèria and Institut de Ciències del Cosmos, Universitat de Barcelona, E-08028 Barcelona, Spain*

[3]*Excited Baryon Analysis Center (EBAC), Thomas Jefferson National Accelerator Facility, Newport News, Virginia 22901, USA*

[4]*Physics Division, Argonne National Laboratory, Argonne, Illinois 60439, USA*

[5]*Department of Physics, Osaka University, Toyonaka, Osaka 560-0043, Japan*

(Received 22 April 2008; published 6 August 2008)

The reaction $\pi^- p \to \eta n$ is investigated within a dynamical coupled-channels model of meson production reactions in the nucleon resonance region. The meson baryon channels included are $\pi N$, $\eta N$, $\pi\Delta$, $\sigma N$, and $\rho N$. The nonresonant meson-baryon interactions of the model are derived from a set of Lagrangians by using a unitary transformation method. One or two excited nucleon states in each of $S$, $P$, $D$, and $F$ partial waves are included to generate the resonant amplitudes. Data of the $\pi^- p \to \eta n$ reaction from threshold up to a total center-of-mass energy of about 2 GeV are satisfactorily reproduced and the roles played by the following nine nucleon resonances are investigated: $S_{11}(1535)$, $S_{11}(1650)$, $P_{11}(1440)$, $P_{11}(1710)$, $P_{13}(1720)$, $D_{13}(1520)$, $D_{13}(1700)$, $D_{15}(1675)$, and $F_{15}(1680)$. The reaction mechanism and the predicted $\eta N$ scattering length are discussed.

DOI: 10.1103/PhysRevC.78.025204 PACS number(s): 11.80.−m, 13.75.−n, 24.10.Eq

## I. INTRODUCTION

In spite of the quasiextinction of pion beams facilities about two decades ago, we are witnessing a growing interest in theoretical investigations of pion-nucleon ($\pi N$) interactions. This is mainly due to the well-recognized fact [1,2] that the impressive amount of high-quality data on electromagnetic meson production reactions from several facilities (ELSA, GRAAL, JLab, LEPS, and MAMI) can be used to pin down the underlying reaction mechanisms and to study the role and/or properties of intervening baryon resonances only when the corresponding hadronic production reactions can also be consistently understood. The present work is a prelude to a comprehensive study of the process $\gamma p \to \eta p$, where, regardless of the direct production mechanisms considered, a meaningful determination of the resonance properties from the $\eta$ photoproduction data requires the inclusion of intermediate- and final-state meson-nucleon interactions. This latter task is tackled in the present work by analyzing the world data of the $\pi^- p \to \eta n$ reaction.

To see the main features of our approach, it is useful to briefly describe here some of the recent theoretical works that account for $\pi^- p \to \eta n$ reaction data. The K-matrix coupled-channels approach by Sauermann *et al.* [3] included only $\pi N$ and $\eta N$ channels and was limited to the $S_{11}$ partial wave. Such a K-matrix approach was then extended by Green and Wycech [4] to include the $\gamma N$ channel in a combined analysis of both $\pi^- p \to \eta n$ and $\gamma p \to \eta p$ reactions, and more extensively developed by the Giessen group [5–7] to include $\pi N$, $\eta N$, $\pi\pi N$, $\omega N$, $K\Lambda$, and $K\Sigma$ channels. The approach developed by the Bonn group [8,9] is also a K-matrix coupled-channels model supplemented with Regge phenomenology. The approach taken by the Zagreb group [10–13] has concentrated on performing the partial-wave analysis of $\pi N \to \pi N, \eta N$ reaction data. This latter approach is most extensively developed by the Virginia Polytechnic Institute-George Washington University (SAID) group [14] and is regularly updated. In an approach based on the Carnegie Melon University-Berkeley (CMB) model, the Pittsburgh-Argonne Collaboration [15,16] also has performed a partial-wave analysis of the $\pi N \to \eta N$ reaction, which is needed in their extraction of nucleon resonance parameters using the method of analytic continuation. Apart from using a simple distant-pole parametrization of the nonresonant interactions, that approach is not far from the dynamical coupled-channel model employed in this work. Detailed discussions on the differences among the K-matrix models, the models of the Pittsburgh-Argonne Collaboration, and that of the Zagreb group are given in Ref. [16].

In this work, we start with a dynamical coupled-channels model, which is based on a Hamiltonian formulation [2] and was applied [17] to analyze $\pi N$ elastic scattering data. This theoretical framework, embodying the $\pi N$, $\eta N$, $\pi\Delta$, $\sigma N$, and $\rho N$ channels, is an extension of the approach of Ref. [18] and is rather different from the models just described, as discussed in detail in Refs. [2,17]. Qualitatively speaking, the K-matrix approaches, which can be derived [1] from a dynamical formulation by taking the on-shell approximation, avoid an explicit treatment of the reaction mechanisms in the short-range region, where we want to map out the quark-gluon substructure of the excited states ($N^*$) of the nucleon. Such a simplification in interpreting the data is also not taken in other dynamical approaches such as those developed recently in Refs. [19–21] and the earlier works reviewed in Ref. [1]. Besides the approaches mentioned, attempts [22,23] to introduce subnucleonic degrees of freedom in studying the $\pi^- p \to \eta n$ reaction are also becoming available.

Moreover, combining the dynamical coupled-channels approach and the constituent quark model approach [24] to study [25–27] the $\gamma p \to K^+\Lambda$ process proves to be a useful step in deepening our understanding of baryon spectroscopy and in searching for missing nucleon resonances [28].

 

This work follows closely the model (JLMS) developed [17] in a study of $\pi N$ elastic scattering. The relevant scattering equations are described in Sec. II. Section III is devoted to the model building procedure and evaluation of the database. We also present our results for differential and total cross sections of the $\pi^- p \to \eta n$ process, in the center-of-mass energy range $W \lesssim 2$ GeV, and discuss the main features of the considered reaction mechanism. In Sec. IV the ingredients of the constructed model are used to predict the $\eta N$ scattering length, as well as the total cross section for the $\eta p \to \eta p$ process. A summary and conclusions are given in Sec. V.

## II. THEORETICAL FRAMEWORK

A detailed description of the coupled-channels formalism can be found in Refs. [2,17]. We outline here the main ingredients necessary to understand the procedure followed in the present work.

The meson baryon ($MB$) transition amplitudes in each partial wave can be written as

$$T_{MB,M'B'}(E) = t^{\rm NR}_{MB,M'B'}(E) + t^{R}_{MB,M'B'}(E), \tag{1}$$

where

$$MB \equiv \pi N, \eta N, \pi\Delta, \rho N, \sigma N. \tag{2}$$

The full amplitudes $T_{MB,M'B'}(E)$ can be directly used to calculate $MB \to M'B'$ scattering observables. The nonresonant amplitude $t^{\rm NR}_{MB,M'B'}(E)$ in Eq. (1) is defined by the coupled-channels equations

$$t^{\rm NR}_{MB,M'B'}(E) = V_{MB,M'B'}(E) + \sum_{M''B''} V_{MB,M''B''}(E) \times G_{M''B''}(E)\, t^{\rm NR}_{M''B'',M'B'}(E), \tag{3}$$

with $G_{M''B''}(E)$ meson-baryon propagators and

$$V_{MB,M'B'}(E) = v_{MB,M'B'} + Z^{(E)}_{MB,M'B'}(E). \tag{4}$$

The interactions $v_{MB,M'B'}$ are derived from tree-level processes by using a unitary transformation method. They are energy independent and free of singularities. However, $Z^{(E)}_{MB,M'B'}(E)$ is induced by the decays of the unstable particles ($\Delta$, $\rho$, $\sigma$) and thus contains *moving* singularities owing to the $\pi\pi N$ cuts. As emphasized in Ref. [17], we neglect that term at this stage.

The second term in the right-hand-side of Eq. (1) is the resonant term defined by

$$t^{R}_{MB,M'B'}(E) = \sum_{N^*_i,N^*_j} \bar{\Gamma}_{MB\to N^*_i}(E)[D(E)]_{i,j}\bar{\Gamma}_{N^*_j\to M'B'}(E), \tag{5}$$

with the $N^*$ propagator

$$[D^{-1}(E)]_{i,j} = \left(E - M^0_{N^*_i}\right)\delta_{i,j} - \bar{\Sigma}_{i,j}(E), \tag{6}$$

where $M^0_{N^*}$ is the bare mass of the resonant state $N^*$, and the self-energies are

$$\bar{\Sigma}_{i,j}(E) = \sum_{MB} \Gamma_{N^*_i\to MB} G_{MB}(E) \bar{\Gamma}_{MB\to N^*_j}(E). \tag{7}$$

The dressed vertex interactions in Eqs. (5) and (7) are (where we define $\Gamma_{MB\to N^*} = \Gamma^{\dagger}_{N^*\to MB}$)

$$\bar{\Gamma}_{MB\to N^*}(E) = \Gamma_{MB\to N^*} + \sum_{M'B'} t^{\rm NR}_{MB,M'B'}(E) G_{M'B'}(E)\Gamma_{M'B'\to N^*}, \tag{8}$$

$$\bar{\Gamma}_{N^*\to MB}(E) = \Gamma_{N^*\to MB} + \sum_{M'B'} \Gamma_{N^*\to M'B'} G_{M'B'}(E) t^{\rm NR}_{M'B',MB}(E). \tag{9}$$

The parametrization used for $\Gamma_{N^*,MB}$ is explained in Ref. [17].

The meson-baryon propagators $G_{MB}$ in these equations are

$$G_{MB}(k, E) = \frac{1}{E - E_M(k) - E_B(k) + i\epsilon} \tag{10}$$

for the stable particle channels $MB \equiv \pi N, \eta N$ and

$$G_{MB}(k, E) = \frac{1}{E - E_M(k) - E_B(k) - \Sigma_{MB}(k, E)} \tag{11}$$

for the unstable particle channels $MB \equiv \pi\Delta, \rho N, \sigma N$. The self-energies in Eq. (11) are computed explicitly as defined in Ref. [17].

To solve the coupled-channels equations, Eq. (3), we need to regularize the matrix elements of $v_{MB,M'B'}$. We include at each meson-baryon-baryon vertex a form factor of the following form:

$$F(\vec{k}, \Lambda) = \left[\frac{\vec{k}^2}{\vec{k}^2 + \Lambda^2}\right]^2, \tag{12}$$

with $\vec{k}$ being the meson momentum. For the meson-meson-meson vertex of $v^t$, the form factor in Eq. (12) is also used with $\vec{k}$ being the momentum of the exchanged meson. For the contact term $v^c$, we regularize it by $F(\vec{k}, \Lambda)F(\vec{k}', \Lambda')$. Here we follow Ref. [17] and use the parameter values determined there for all nonresonant terms except the ones explicitly mentioned in the following sections.

With the nonresonant amplitudes generated from solving Eq. (3), the resonant amplitude $t^{R}_{MB,M'B'}$ in Eq. (5) then depends on the bare mass $M^0_{N^*}$ and the bare $N^* \to MB$ vertex functions. The vertex functions are parametrized in the following way:

$$\Gamma_{N^*,MB(LS)}(k) = \frac{1}{(2\pi)^{3/2}}\frac{1}{\sqrt{m_N}} C_{N^*,MB(LS)} \times \left[\frac{\Lambda^2_{N^*,MB(LS)}}{\Lambda^2_{N^*,MB(LS)} + (k - k_R)^2}\right]^{(2+L)} \left[\frac{k}{m_\pi}\right]^L, \tag{13}$$

where $L$ and $S$ are the orbital angular momentum and the total spin of the $MB$ system, respectively. $C_{N^*,MB(LS)}$ measure the meson-nucleon-$N^*$ coupling strength for a specific $LS$ combination of the $MB$ system and are treated as free parameters, and the $k_R$ are parameters fixed by the $\pi N \to \pi N$ analysis in Ref. [17]. This parametrization accounts for the threshold $k^L$ dependence and the right power $(2 + L)$ such that the integration for calculating the dressed vertex Eqs. (8) and (9) is finite.

## III. RESULTS AND DISCUSSION

The world database for the process under investigation embodies 1508 differential and 98 total cross sections [29–37] for $1.47 \leqslant W \leqslant 2.85$ GeV. However, those data presented in 12 papers, theses, and reports have been obtained mainly between 1964 and 1980, except for recent results from the Brookhaven National Laboratory and using the Crystal Ball detector by Morrison [29] and Prakhov *et al.* [30]. The quality of data obtained before 1980 has been discussed by Clajus and Nefkens [38] and, as emphasized by George Washington University (GWU) [14], Zagreb [10], and Giessen [6,7] groups, there are underlying inconsistencies among different data sets, because of experimental shortcomings and the underestimate of systematic uncertainties. This uncomfortable situation has led various authors to use a reduced database. For example, the GWU group [14] includes in the database 257 data points, mainly from differential cross-section measurements [29–32], but also about 50 data points for total cross sections [29,31,32,35,37].

In the present work, we concentrate only on the differential cross sections for $W \lesssim 2$ GeV, as summarized in Table I. The number of data points included in the fitted database in this work (294) will be discussed in Sec. III A.

One of the delicate points in dealing with those data is related to the systematic uncertainties ($\delta_{\rm sys}$). For the most recent data by Prakhov *et al.* [30] those uncertainties are given clearly by the authors (6%). For old data, we have mainly followed the general trend suggested in Ref. [38], as summarized in the last column of Table I. Deinet *et al.* [31] report two sources of systematic uncertainty: 7% and 9%, to be added up quadratically, giving $\delta_{\rm sys} = 11.4\%$. For Richards *et al.* [32], we have used $\delta_{\rm sys} = 10\%$ for the lowest energies and 11% to 14% for other ones, as given in the original paper. For Debenham *et al.* [33] and Brown *et al.* [34], we have followed the conclusion of the Zagreb group [10,12]. In the case of Brown *et al.* [34], we also have lowered the momentum by 4%, in line with Ref. [38].

Total cross-section data have not been included in our fits for the following reasons: (i) Differential cross sections are measured by various collaborations in significantly different angular ranges with respect to extreme ones (see the second column in Table I), (II) there is no commonly agreed upon procedure to extract total cross sections from measured angular distributions, and (iii) model predictions for extreme angles do not in general agree with each other.

### A. Fitting procedure

As already mentioned, in Ref. [17] the $\pi N \to \pi N$ reaction was studied within a coupled-channels formalism, with multistep processes embodying $\pi N$, $\eta N$, $\pi\Delta$, $\sigma N$, and $\rho N$ states.

In that work 175 adjustable parameters were introduced to fit amplitudes produced by the SAID group, fitting more than 10,000 data points. About 30 of those parameters are particularly relevant to the coupled-channels mechanisms for the $\pi^- p \to \eta n$ reaction. Accordingly, in the present work we use that reduced set of adjustable parameters (see Table II) and fix the others to their values as determined in Ref. [17] (cf. Tables III to VII in that paper). A total of 294 data points are fitted in the present work (see Table I). Here, we comment on the exclusion of a few data points in Ref. [30] from the fitted database. Actually, as previously mentioned, on the one hand, recent data by Prakhov *et al.* [30] bear much smaller errors than other data, and, on the other hand, the database suffers from some inconsistencies. One of the consequences of this situation is that a few data points introduce large $\chi^2$ values (around 10 or more), thus reducing significantly the efficiency of the minimization procedure. The excluded points concern mainly the two lowest energy sets of Ref. [30].

In the following we present our results for two models, as well as those obtained using the parameters reported in Ref. [17] (see Table II and Figs. 1 and 2). Here, in line with Ref. [17], the following nucleon resonances ($N^*$) are considered: $S_{11}(1535)$, $S_{11}(1650)$, $P_{11}(1440)$, $P_{11}(1710)$, $P_{13}(1720)$, $D_{13}(1520)$, $D_{13}(1700)$, $D_{15}(1675)$, and $F_{15}(1680)$.

The adjustable parameters for nonresonant terms are the $\eta NN$ coupling constant $f_{\eta NN}$ and cutoff $\Lambda_{\eta NN}$. For resonant terms the parameters are as follows: $N^*$ bare masses $M_0^{N^*}$, $\eta NN^*$ coupling strengths $C_{\eta NN^*}$, and cutoffs $\Lambda_{\eta NN^*}$.

Model *A* is obtained by fitting the database and those 29 adjustable parameters (see column 3 in Table II). Model *B*, for reasons explained in the following, has five more adjustable parameters, namely, the coupling constants and cutoffs of $\rho N S_{11}$, with $S_{11} \equiv S_{11}(1535)$ and $S_{11}(1650)$ for $[LS] = [0, 1/2]$, as well as the cutoff $\Lambda_{\rho N S_{11}(1535)}$ for $[LS] = [2, 3/2]$. Finally, for comparisons, we reproduce in Table II the relevant

TABLE I. Summary of differential cross-section data for the reaction $\pi^- p \to \eta n$. Data sets investigated in the present work are singled out in the last two columns, where the number of data points ($N_{\rm dp}$) per data set used in the fitting procedure is given.

| Reference | Angular range (Degrees) | $P_\pi$ (GeV/$c$) | $W$ (GeV) | $N_{\rm dp}$ | $N_{\rm dp}$ used in the the present work | $\delta_{\rm sys}$ |
|---|---|---|---|---|---|---|
| Prakhov *et al.* [30] | 23–157 | 0.687–0.747 | 1.49–1.52 | 84 | 70 | 6% |
| Deinet *et al.* [31] | 32–123 | 0.718–1.050 | 1.51–1.70 | 83 | 80 | 11% |
| Richards *et al.* [32] | 26–154 | 0.718–1.433 | 1.51–1.90 | 70 | 66 | 10% to 14% |
| Debenham *et al.* [33] | 162–172 | 0.697–0.999 | 1.49–1.67 | 111 | 27 | 10% + 0.02 mb |
| Brown *et al.* [34] | 18–160 | 0.724–2.724 | 1.51–2.45 | 379 | 51 | 10% or 0.01 mb |
| Morrison [29] | 46–134 | 0.701–0.747 | 1.50–1.52 | 34 | – | |
| Crouch *et al.* [35] | 14–167 | 1.395–3.839 | 1.88–2.85 | 731 | – | |
| Feltesse *et al.* [36] | 20–160 | 0.757 | 1.53 | 16 | – | |

TABLE II. Parameters for models $A$ and $B$ determined in this work. The last column gives the values determined in Ref. [17].

| Category | Parameter | Model $A$ | Model $B$ | Ref. [17] |
|---|---|---|---|---|
| Nonresonant $\eta N$ parameters | | | | |
| | $f_{\eta NN}$ | 4.9936 | 4.9999 | 3.8892 |
| | $\Lambda_{\eta NN}$ | 592.11 | 591.91 | 623.56 |
| Bare mass $M_0^{N^*}$ | | | | |
| | $S_{11}(1535)$ | 1809 | 1808 | 1800 |
| | $S_{11}(1650)$ | 1901 | 1861 | 1880 |
| | $P_{11}(1440)$ | 1775 | 1784 | 1763 |
| | $P_{11}(1710)$ | 2019 | 2057 | 2037 |
| | $P_{13}(1720)$ | 1726 | 1691 | 1711 |
| | $D_{13}(1520)$ | 1918 | 1919 | 1899 |
| | $D_{13}(1700)$ | 1971 | 1968 | 1988 |
| | $D_{15}(1675)$ | 1878 | 1878 | 1898 |
| | $F_{15}(1680)$ | 2207 | 2207 | 2187 |
| $C_{N^*\to MB(LS)}$ | | | | |
| | $C_{\eta NS_{11}(1535)}$ | 8.4269 | 7.8344 | 9.1000 |
| | $C_{\rho NS_{11}(1535)}$ | *2.0280* | −0.4935 | 2.028 |
| | $C_{\eta NS_{11}(1650)}$ | 2.0487 | −0.4221 | 0.6000 |
| | $C_{\rho NS_{11}(1650)}$ | *−9.5179* | 2.0000 | −9.5179 |
| | $C_{\eta NP_{11}(1440)}$ | 1.6321 | 1.6298 | 2.6210 |
| | $C_{\eta NP_{11}(1710)}$ | 2.4925 | 2.4994 | 3.6611 |
| | $C_{\eta NP_{13}(1720)}$ | 2.4474 | 2.4997 | −0.9992 |
| | $C_{\eta ND_{13}(1520)}$ | 0.4440 | 0.4267 | −0.0174 |
| | $C_{\eta ND_{13}(1700)}$ | −1.8985 | −0.6463 | 0.3570 |
| | $C_{\eta ND_{15}(1675)}$ | 0.2456 | 0.3437 | −0.0959 |
| | $C_{\eta NF_{15}(1680)}$ | −0.0446 | −0.0265 | 0.0000 |
| $\Lambda_{N^*\to MB(LS)}$ | | | | |
| | $\Lambda_{\eta NS_{11}(1535)}$ | 779.38 | 799.90 | 598.97 |
| | $\Lambda_{\rho NS_{11}(1535)}$ | *1999.8* | 670.89 | 1999.8 |
| | | *1893.8* | 955.8 | 1893.8 |
| | $\Lambda_{\eta NS_{11}(1650)}$ | 500.07 | 1999.70 | 500.02 |
| | $\Lambda_{\rho NS_{11}(1650)}$ | *796.83* | 2000.00 | 796.83 |
| | $\Lambda_{\eta NP_{11}(1440)}$ | 1766.80 | 1757.40 | 1654.85 |
| | $\Lambda_{\eta NP_{11}(1710)}$ | 500.08 | 500.00 | 897.84 |
| | $\Lambda_{\eta NP_{13}(1720)}$ | 631.90 | 649.11 | 500.23 |
| | $\Lambda_{\eta ND_{13}(1520)}$ | 500.20 | 500.01 | 1918.20 |
| | $\Lambda_{\eta ND_{13}(1700)}$ | 540.55 | 763.13 | 678.41 |
| | $\Lambda_{\eta ND_{15}(1675)}$ | 507.64 | 500.00 | 1554.00 |
| | $\Lambda_{\eta NF_{15}(1680)}$ | 811.72 | 1073.80 | 655.87 |
| $\chi^2_{\rm dp}$ | | 2.03 | 1.94 | 6.94 |

values reported in Ref. [17]. As mentioned, in that latter work, adjustable parameters are determined via the $\pi N \to \pi N$ channels, and for the $\pi^- p \to \eta n$ reaction the database embodied only a few total cross-section data from Refs. [30,34]. Notice that the five $\rho N S_{11}$ parameters in model $A$ (shown in italics in Table II) were not treated as adjustable parameters and hence are identical to those of Ref. [17].

### B. Differential and total cross sections for the process $\pi^- p \to \eta n$

In Figures 1 and 2 we compare the results of the models $A$ and $B$ with the differential cross-section data, for which the reduced $\chi^2$ values per data point are 2.03 and 1.94, respectively. Those numbers compare well with the GWU [14] reduced $\chi^2 = 2.44$. In the same figures, we also show results obtained by using the parameters of Ref. [17], which gives $\chi^2 = 6.94$.

Before discussing different curves in comparison with data, we wish to emphasize the difference between models $A$ and $B$. Once model $A$ was obtained, we investigated the importance of various parameters and found that by switching off the $\rho$ coupling to the $S_{11}(1535)$, $\chi^2$ increased by roughly a factor of 3. Within the investigated reaction, such a high sensitivity to the $\rho N S_{11}$ seems unrealistic. To eliminate that behavior, we refitted the data by allowing those coupling constants to vary in the range of $\pm 0.5$ for $S_{11}(1535)$ and $\pm 2$ for $S_{11}(1650)$,

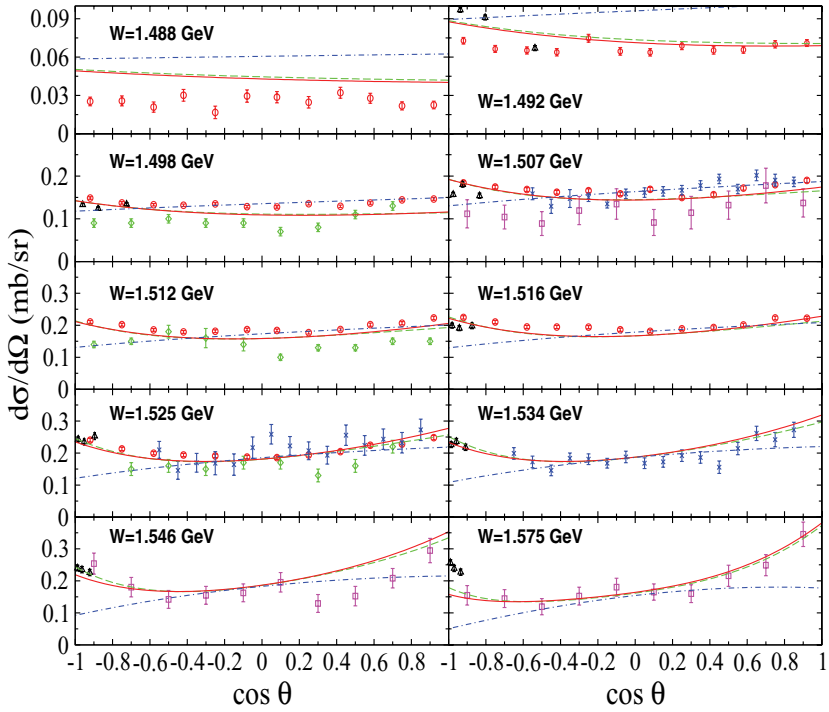


FIG. 1. (Color online) Differential cross section for the reaction $\pi^- p \to \eta n$. The curves correspond to models *A* (dashed) and *B* (full) from the present work. The dash-dotted curves are obtained by using the parameters in Ref. [17]. Data are from Prakhov *et al.* [30] (empty circles), Deinet *et al.* [31] (crosses), Richards *et al.* [32] (empty squares), Debenham *et al.* [33] (up triangles), and Morrison [29] (diamonds). Data uncertainties depicted are only statistical ones.

instead of $\pm 10$. Model *B* is then obtained, where that effect is significantly reduced. Comparing the two models in Figs. 1 and 2, we observe that they differ from each other by less than the statistical uncertainties of the data, corroborating that the $\pi^- p \to \eta n$ reaction is not a proper channel to pin down those couplings. Better constraints on those couplings can be obtained by investigating the $\pi N \to \pi\pi N$ process [39].

Models *A* and *B* show reasonable agreements with Prakhov *et al.* [30] data, except at the lowest energy (Fig. 1). We will return to that point later. Data from Morrison [29] are also depicted at four common energies. That latter data set, not included in our fitting procedure, shows systematically smaller cross sections compared to Ref. [30] data.

The Prakhov *et al.* [30] data set at $W = 1.507$ GeV is of special interest, since there are also data from three other measurements. Results from Deinet *et al.* [31] are compatible with Prakhov *et al.* data, though with larger uncertainties (which become even more sizable at $W = 1.525$ GeV). The Richards *et al.* [32] data show deviations from Prakhov *et al.*

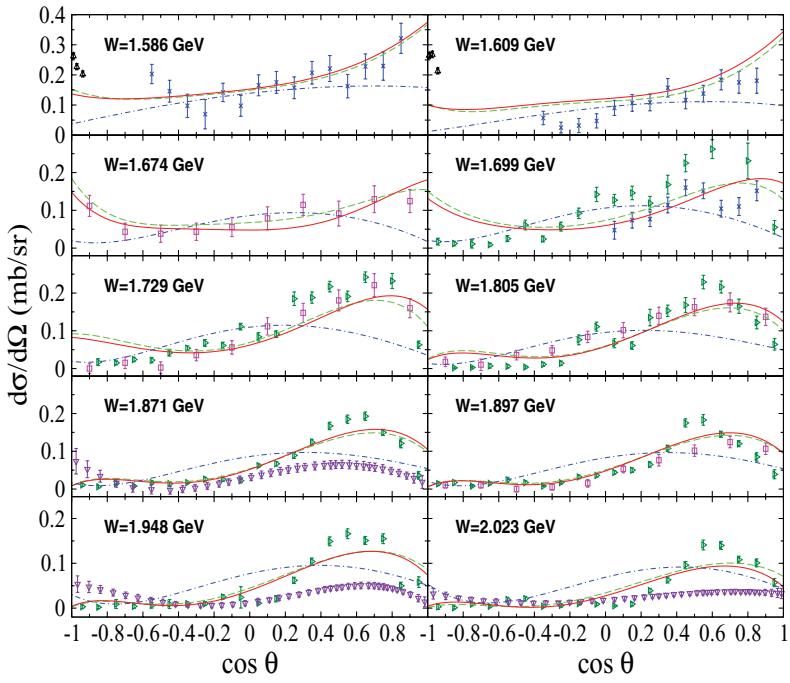


FIG. 2. (Color online) Differential cross section for the reaction $\pi^- p \to \eta n$. Curves and data are as in Fig. 1. Additional data are from Brown *et al.* [34] (right triangles) and Crouch *et al.* [35] (down triangles).

ones, especially at most backward angles. Finally, copious data from Debenham *et al.* [33] are unfortunately limited to extreme backward angles and appear to be rather consistent with other data only up to $W \approx 1.55$ GeV. This trend is confirmed in Fig. 2, where models *A* and *B* reproduce correctly results from Deinet *et al.* [31] and Richards *et al.* [32]. Both sets of data come out fairly compatible with measurements from Brown *et al.* [34] at $W = 1.699$, 1.729, and 1.805 GeV. Models *A* and *B* show acceptable agreements with those data, except at backward angles, where the model/experiment discrepancies get reduced when energy increases and suitable agreement is observed at $W = 1.897$ GeV. At the three remaining depicted energies ($W = 1.871$, 1.948, and 2.003 GeV) our models reproduce the general trend of the Brown *et al.* data. At those energies, data from Crouch *et al.* [35], not included in our database, are also shown. The two data sets are not consistent. Given the known problems [38] with Brown's data, we also attempted to fit the database, within model *A*, by replacing the Brown *et al.* data by those of Crouch *et al.* at $W = 1.879$ and 1.915 GeV. However, we observed a significant increase of $\chi^2$, which goes from 2.03 to 4.12, and with very undesirable effects in the Crystal Ball energy range.

In Figures 1 and 2, results using the parameters in Ref. [17] are also shown. At lowest energies, that model overestimates the data. At higher energies, it shows significant deviations, first at backward angles and then at forward angles. Above $W \approx 1.8$ GeV it tends to miss the data.

Finally, as previously mentioned, we did not include the extracted total cross-section data in our database. In Fig. 3, we show the postdictions of our models *A* and *B*, as well as results of the Ref. [17], and compare them with the data. Both models *A* and *B* reproduce the data correctly, except for those by Crouch *et al.* [35], for which the differential cross sections turn out to be significantly smaller than other data, as shown in Fig. 2. Moreover, the background contributions show a smooth behavior and are small with respect to the full model results, except around the minimum of the total cross section, where resonant terms produce highly destructive interference.

To conclude, we wish to emphasize that the results of Ref. [17] are extended to the process $\pi^- p \to \eta n$ and two models are obtained, reproducing equally well the general

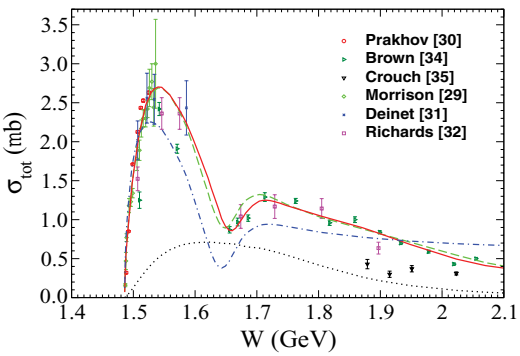


FIG. 3. (Color online) Total cross section for the reaction $\pi^- p \to \eta n$. Curves are from Ref. [17] (dash-dotted), model *A* (dashed), model *B* (full), and the background contributions (dotted) in model *B*. Data are as in Figs. 1 and 2.

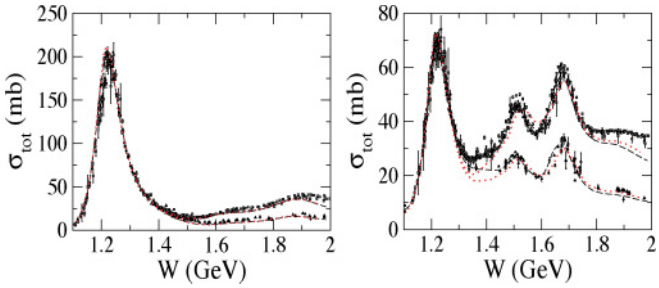


FIG. 4. (Color online) Comparisons between the results from Ref. [17] (dashed curves) and model *B* (dotted curves) for $\pi N \to X, \pi N$ processes. Left panel: Predicted total cross section for the reactions $\pi^+ p \to X$ (upper set) and $\pi^+ p \to \pi^+ p$ (lower set). Right panel: Predicted total cross section for the reactions $\pi^- p \to X$ (upper set) and $\pi^- p \to \pi^- p + \pi^\circ n$ (lower set). Data in both panels are from Refs. [40,41].

features of a heterogeneous database. This new set of parameters, particularly relevant to the investigated process, does not spoil the excellent results obtained in Ref. [17], which are devoted mainly to the $\pi N \to \pi N$ observables. To illustrate this latter point, results from Ref. [17] and our model *B* are shown in Fig. 4, where Figs. 13 and 14 of Ref. [17] have been complemented with the predictions of the model *B*. For the processes with $\pi^+ p$ initial state (left panel in Fig. 4), results from the two models overlap with each other. For reactions involving $\pi^- p$ initial states (right panel in Fig. 4), model *B* gives deeper minima around $W \approx 1.4$ GeV than those reported in Ref. [17], with the largest discrepancy between the two curves being less than 20%.

### C. Partial-wave amplitudes

To make clear the impact of the present work on the partial-wave amplitudes reported in Ref. [17], we present the T matrix for each partial wave,

$$T_{\pi N \to MN} = -\pi k \frac{\sqrt{k^2 + m_N^2}\sqrt{k^2 + m_\pi^2}}{\sqrt{k^2 + m_N^2} + \sqrt{k^2 + m_\pi^2}} t_{MN}(k, k'), \quad (14)$$

with $M \equiv \pi$ for the $\pi N \to \pi N$ process. We also produce results for the $\pi N \to \eta N$ reaction ($M \equiv \eta$).

The real and imaginary parts of the *S*, *P*, *D*, and *F* partial-wave amplitudes are depicted in Figs. 5 and 6, respectively. The corresponding results from models *A* and *B* of this paper (see Table II) are compared to the model reported in Ref. [17] and to the energy-independent solution of the SAID partial-wave analysis [42].

The comparison to the model of Ref. [17] reflects the importance of the constraints imposed in our work, namely, the use of $\pi N \to \eta N$ scattering data to further constrain the $\pi N \to \pi N$ sector. The partial-wave amplitudes most affected are $S_{11}$, $P_{11}$, and $P_{13}$, reflecting the main trends of the reaction mechanism found in the present work, as discussed in the next section. The $S_{11}$ partial wave in the $W = 1.535$ GeV region is different from that of the model of Ref. [17]. This is expected as the coupling of the $N(1535) \to \eta N$ is known to be large

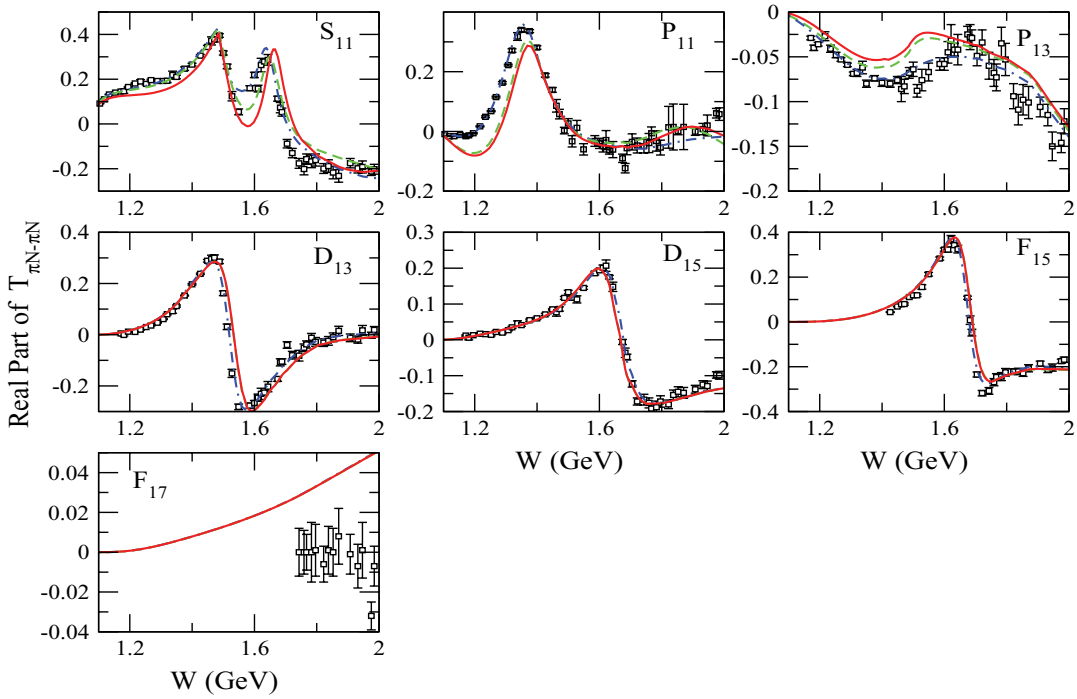


FIG. 5. (Color online) Real parts of the calculated $\pi N \to \pi N$ T matrices of isospin 1/2 for $l \leqslant 3$ partial waves as a function of total c.m. energy. Results from model $A$ (dashed curves), model $B$ (full curves), and Ref. [17] (dash-dotted) are compared with the solutions of Ref. [42] (empty squares).

and thus very important in the $\pi N \to \eta N$ phenomenology considered in the present paper. For the $P_{11}$ both models, $A$ and $B$, produce a similar behavior for the real part of the amplitude, which however peaks around the same energy value of $\sim$1.400 GeV. For the $P_{13}$ wave, the largest deviations between our models and that of Ref. [17] are around $W \approx 1.6$ GeV. The higher partial waves show no significant sensitivities to the new set of parameters.

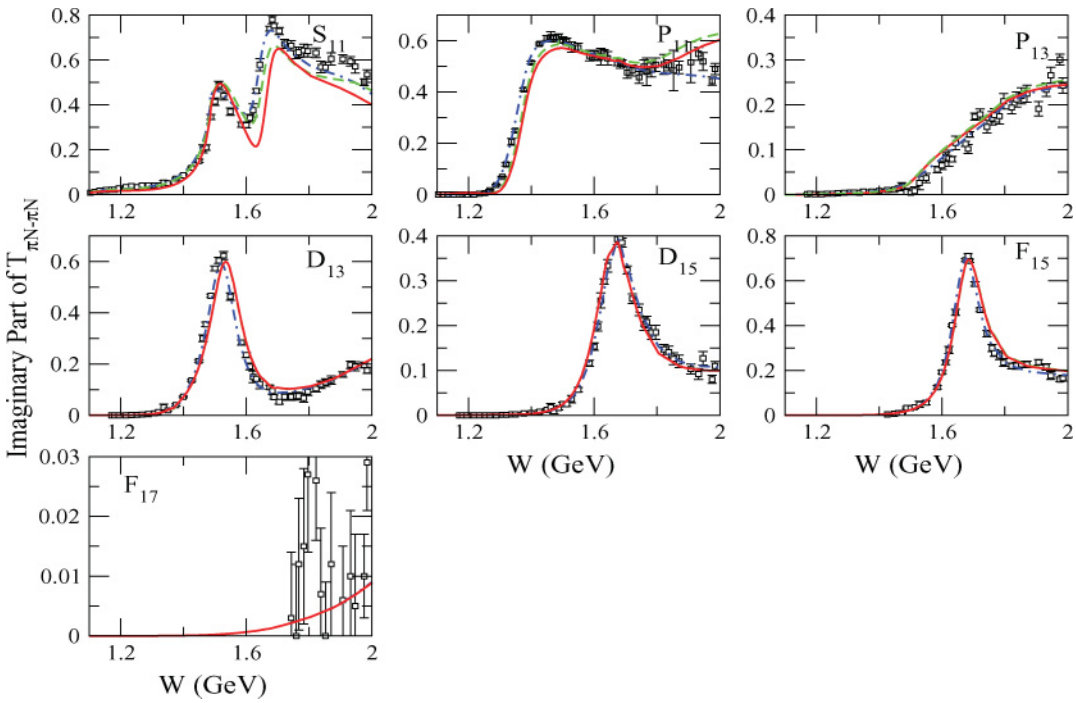


FIG. 6. (Color online) The same as Fig. 5, but for the imaginary parts.

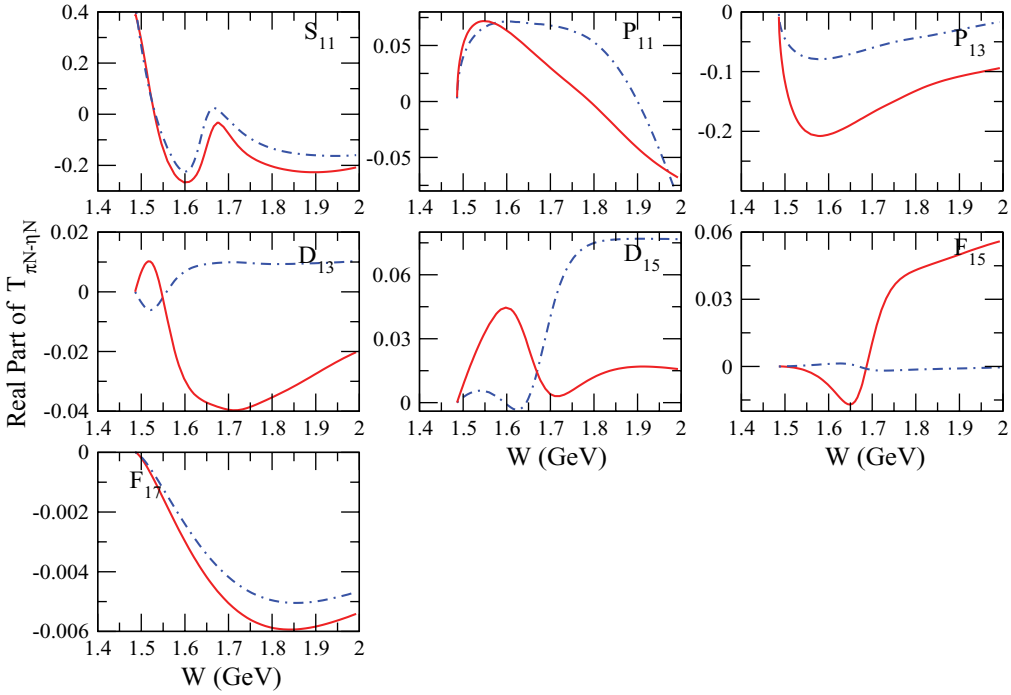


FIG. 7. (Color online) Real parts of the calculated $\pi N \to \eta N$ T matrices for $l \leqslant 3$ partial waves as a function of total c.m. energy. Results are from model $B$ (full curves) and Ref. [17] (dash-dotted curves).

We end this section by reporting in Figs. 7 and 8 our results from model $B$ for the process $\pi^- p \to \eta n$ and compare them with the outcome of Ref. [17]. Both models produce similar results for the dominant $S_{11}$ and the marginal $F_{17}$ partial-wave real and imaginary parts. For all other partial waves significant discrepancies between the two models are observed. This general trend appears also with respect to the results reported in Refs. [15,16]. To go beyond the $l = 0$ partial wave, extension of the approach in Ref. [17] to other final states, such as $\rho N$ and $\pi\Delta$, is mandatory. As emphasized in Ref. [16], the investigation of the $\pi N \to \pi\pi N$ channel is crucial in extracting partial waves up to at least $l = 4$.

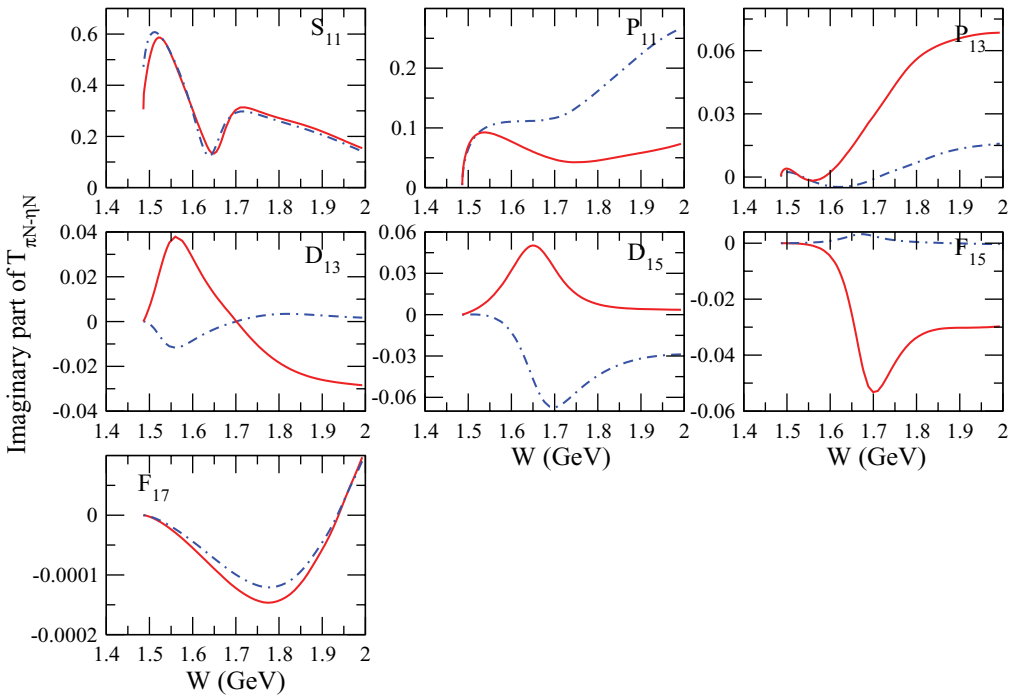


FIG. 8. (Color online) The same as Fig. 7, but for the imaginary parts.

TABLE III. Reduced $\chi^2$ per data point for model $B$ with one resonance switched off (the reduced $\chi^2$ for the full model $B$ being 1.94).

| | $S_{11}(1535)$ | $S_{11}(1650)$ | $P_{11}(1440)$ | $P_{11}(1710)$ | $P_{13}(1720)$ | $D_{13}(1520)$ | $D_{13}(1700)$ | $D_{15}(1675)$ | $F_{15}(1680)$ |
|---|---|---|---|---|---|---|---|---|---|
| $\chi^2$ | 48.86 | 2.62 | 3.55 | 2.37 | 2.77 | 2.23 | 1.93 | 2.10 | 2.47 |

### D. Main features of the $\pi^- p \to \eta n$ reaction mechanism

To gain some insight as to the main ingredients of the reaction mechanism, we concentrate on model $B$. Starting from that model, and without further minimizations, we have checked the variations of the $\chi^2$ by switching off the nine resonances one by one. The results are reported in Table III.

As expected, the process is dominated by the $S_{11}(1535)$ resonance. There are however two other resonances playing non-negligible roles, namely, $P_{11}(1440)$ and $P_{13}(1720)$. Figures 9 and 10 show that the importance of those resonances depends on both angle and energy. The $S_{11}(1535)$ resonance produces more than 80% of the cross section for the Prakhov *et al.* [30] data. Its importance decreases with energy, especially at backward angles, without vanishing. The effect of the $P_{11}(1440)$ resonance becomes visible roughly in the energy range $1.525 \leqslant W \leqslant 1.8$ GeV, with a destructive behavior at most forward angles. Finally, the $P_{13}(1720)$ resonance appears, in the forward hemisphere, around $W \approx 1.6$ GeV, with the highest contributions at $W \approx 1.73$ GeV and its effect remains constructive.

Although the effect of the $D_{13}(1520)$ resonance on $\chi^2$ is small, it is required to produce the right curvature of the curves at low energies.

In conclusion, model $B$ turns out to describe in a satisfactory manner the data set and embodies a simple reaction mechanism. In the following section we hence use that model for further investigations of the $\eta N$ system.

## IV. PREDICTIONS FOR THE $\eta N$ SCATTERING LENGTH AND THE $\eta p \to \eta p$ TOTAL CROSS SECTION

The $\eta N$ scattering amplitude in terms of the t matrix is given by the following relation:

$$f(k) = -\pi \frac{\sqrt{k^2 + m_N^2}\sqrt{k^2 + m_\eta^2}}{\sqrt{k^2 + m_N^2} + \sqrt{k^2 + m_\eta^2}} t_{\eta N}(k, k). \qquad (15)$$

Then, the scattering length reads

$$a_{\eta N} = \lim_{k \to 0} f(k). \qquad (16)$$

Figure 11 shows the real and imaginary parts of the function $f(k)$, for model $B$, and leads to the following value for the scattering length:

$$a_{\eta N} = (0.30 + i0.18)\ \text{fm}. \qquad (17)$$

The efforts of two decades to determine the $\eta N$ scattering length have recently been reviewed by several authors [43–45]. A lower limit on the imaginary part, derived from the optical

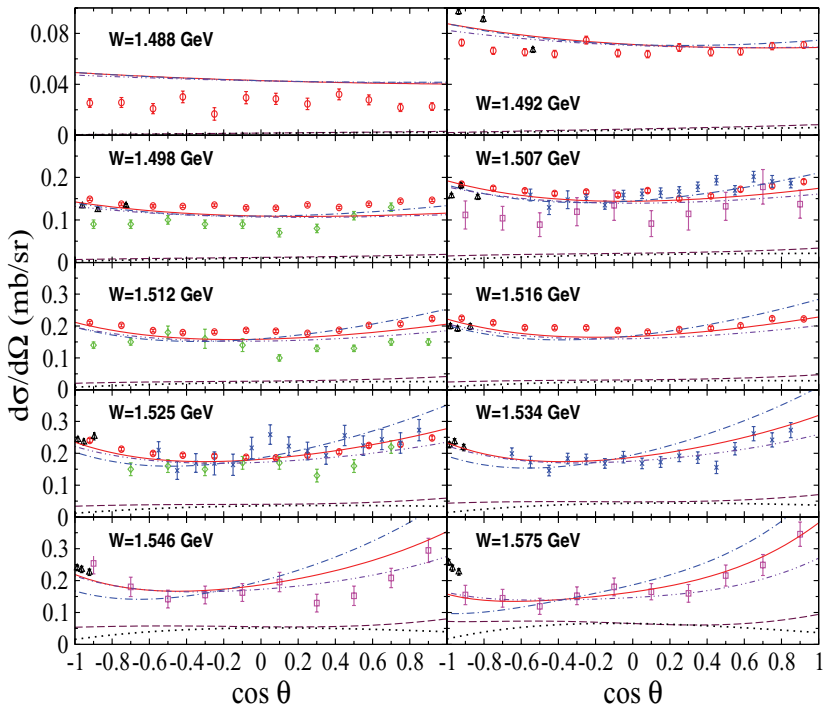


FIG. 9. (Color online) Differential cross section for the reaction $\pi^- p \to \eta n$. The full curves correspond to model $B$ and the dotted ones to contributions from the nonresonant terms. The other curves have been obtained by removing one resonance from that model; the removed resonances are $S_{11}(1535)$ (dashed), $P_{11}(1440)$ (dash-dotted), and $P_{13}(1720)$ (dash-dot-dotted). Data are as in Fig. 1.

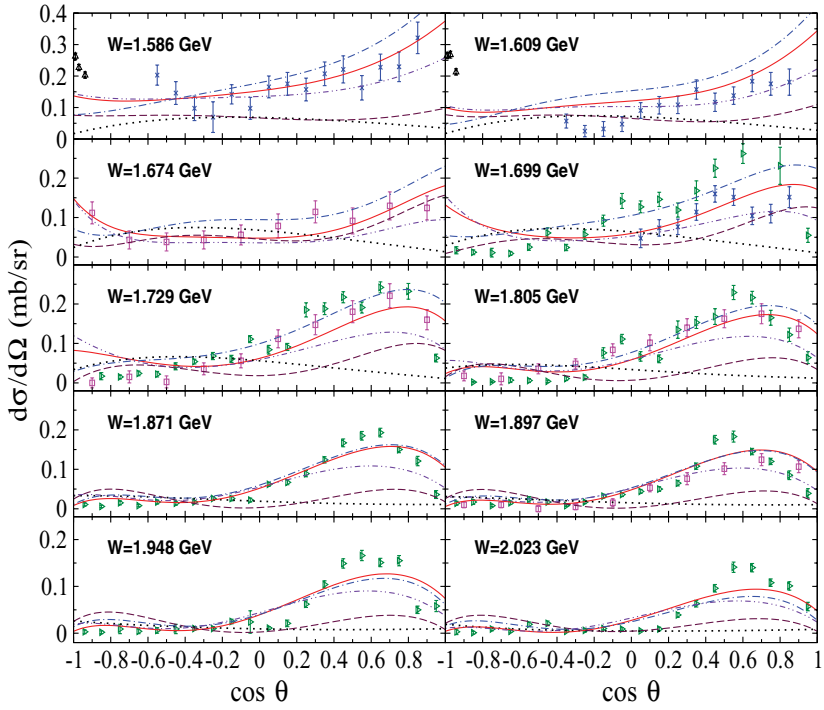


FIG. 10. (Color online) Differential cross section for the reaction $\pi^- p \to \eta n$. The curves are is in Fig. 9. Data are as in Fig. 2.

theorem and taking into account the recent data [29], leads [45] to $0.172 \pm 0.009$ fm. By combining results quoted in those review papers, the present knowledge of the imaginary part is

$$0.17 \lesssim \mathcal{I}m\, a_{\eta N} \lesssim 0.49 \text{ fm}, \tag{18}$$

and our value comes out to be within that range.

For the real part of the scattering length the estimates in the literature give [44]

$$0.27 \lesssim \mathcal{R}e\, a_{\eta N} \lesssim 1.0 \text{ fm}. \tag{19}$$

The value extracted in the present work, within model $B$, is close to the lower limit. Our value is compatible with those obtained via chiral effective Lagrangians [46], the most recent solution (G380) from energy-dependent partial-wave analysis [45] of elastic $\pi^{\pm} p$, $\pi^- p \to \pi^\circ n$, and $\pi^- p \to \eta n$ scattering data, as well as with older findings [47,48]. Investigations based on chiral perturbation approaches [49–51] lead to smaller values of around 0.2 fm. Finally, coupled-channels calculations within the T matrix [10,11,52] or K matrix [53] produce larger values, $0.5 \lesssim \mathcal{R}e\, a_{\eta N} \lesssim 1.0$ fm.

Besides the process $\pi N \to \eta N$, $\eta$ production using proton or deuteron beams has also been investigated by using various sets of $\eta N$ scattering lengths reported in the literature, as summarized in the following:

(i) $pn \to \eta d$ near-threshold data [54] has been studied within a two-step model [48], embodying meson-exchange and final-state $\eta N$ interactions, and favors small scattering length: $a_{\eta N} = (0.29 + i0.36)$ fm. In a microscopic three-body approach in its nonrelativistic version [55] it was concluded that the data are well reproduced by using the results from Ref. [49], $a_{\eta N} = (0.42 + i0.34)$ fm. The relativistic version of that approach [56] shows the importance of initial- and final-state treatments, emphasized also by the Jülich

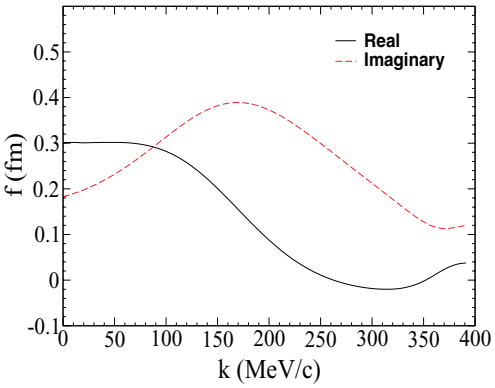


FIG. 11. (Color online) $\eta N$ scattering amplitude $f(k)$ as a function of c.m. momentum, within model $B$.

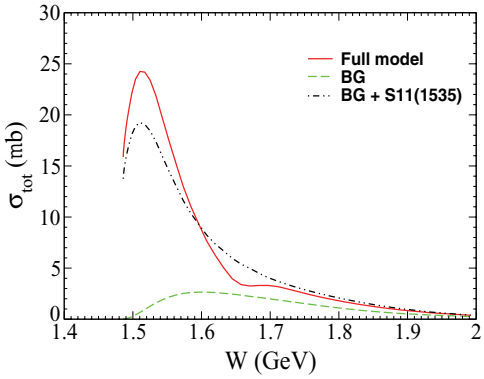


FIG. 12. (Color online) Total cross section for the reaction $\eta p \to \eta p$ as a function of total c.m. energy, within model $B$.

group [57], leading to a reduced selectivity on the sets used for the scattering length.

(ii) $pp \to pp\eta$ [58] and $pn \to pn\eta$ [54] data, as well as the aforementioned data have recently been studied within an effective Lagrangian model [59], resulting in a reasonable account of data for $a_{\eta N} = (0.51 + i0.26)$ fm.

(iii) $\eta$ production in proton-deuteron collisions is being studied [60], but at the present time those investigations do not allow refinements in determining the $\eta N$ scattering length.

The findings of various approaches with respect to the $\eta N$ scattering length, as summarized here, lead then to the ranges for real and imaginary parts as reported in Eqs. (18) and (19). Our value for the real part being close to the lower bound excludes the existence of bound $\eta$-nucleus states.

Finally, we show our prediction for the $\eta N$ elastic scattering total cross section (Fig. 12). The background contributions (dashed curve) turns out to be small and smoothly varying. This latter contribution completed by that of the $S_{11}(1535)$ resonance (dash-dot-dotted curve) accounts for a significant portion of the total cross section predicted by the full model $B$ (full curve).

## V. SUMMARY AND CONCLUSIONS

A dynamical coupled-channels formalism is used to study the the process $\pi^- p \to \eta n$ in the total center-of-mass energy range $W \lesssim 2$ GeV. The formalism embodies, besides nonresonant terms, five intermediate meson-nucleon states, namely, $\pi N$, $\eta N$, $\pi\Delta$, $\sigma N$, and $\rho N$.

Within this phenomenological approach, 34 adjustable parameters are introduced, 2 of them for the nonresonant mechanisms and the others for the 9 nucleon resonances retained in the model search, namely, $S_{11}(1535)$, $S_{11}(1650)$, $P_{11}(1440)$, $P_{11}(1710)$, $P_{13}(1720)$, $D_{13}(1520)$, $D_{13}(1700)$, $D_{15}(1675)$, and $F_{15}(1680)$. That set of resonances corresponds to all known three and four star resonances relevant to the energy range investigated here.

To determine the parameters and build a model, a data set including 294 measured differential cross sections, coming from five collaborations, are fitted. The selection of data points allows us to suppress the manifestations of inconsistencies among available data sets. Our model $B$ reproduces satisfactorily the data, with a reduced $\chi^2 = 1.94$. A detailed study of the reaction mechanism within model $B$ allows a hierarchy in the roles played by nucleon resonances to be established. Actually, the dominant resonance turns out to be the $S_{11}(1535)$. The other resonances affecting $\chi^2$ by more than 20% when switched off are, by decreasing importance, $P_{11}(1440)$, $P_{13}(1720)$, $S_{11}(1650)$, $F_{15}(1680)$, $P_{11}(1710)$, and $D_{13}(1520)$. Contributions from $D_{13}(1700)$ and $D_{15}(1675)$ are found to be negligible.

Model $B$ is used to extract the $\eta N$ scattering length, which comes out to be $a_{\eta N} = (0.30 + i0.18)$ fm. Both the real and imaginary parts of that quantity are within the ranges determined from other works.

To improve our knowledge of the $\pi^- p \to \eta n$ process, and consequently of the $\eta N$ system, further measurements, including polarized target asymmetry, are highly desirable. Such experimental results are expected from existing and/or forthcoming pion beams in the following labs: GSI [61], ITEP [62], Fermi Lab [63], and JPARC [64].

Finally, to take advantage of copious $\eta$ electromagnetic production data, the obtained model $B$ appears reliable enough for our in-progress investigation of the $\gamma p \to \eta p$ reaction within a coupled-channels approach and a constituent quark model [65].

## ACKNOWLEDGMENTS

We are grateful to Bill Briscoe and Ben Nefkens for enlightening discussions on the status of data. The authors thankfully acknowledge the computer resources, technical expertise, and assistance provided by the Barcelona Supercomputing Center—Centro Nacional de Supercomputacion (Spain) and NERSC (USA). B.J.-D. thanks the members of the nuclear theory group at Osaka University for their warm hospitality. This work is partially supported by Grant No. FIS2005-03142 from MEC (Spain) and FEDER and the European Hadron Physics Project No. RII3-CT-2004-506078, by the U.S. Department of Energy, Office of Nuclear Physics Division, under Contract No. DE-AC02-06CH11357 and Contract No. DE-AC05-060R23177, under which Jefferson Science Associates operates Jefferson Lab, and by the Japan Society for the Promotion of Science, Grant-in-Aid for Scientific Research (c)20540270. B.J.-D. acknowledges the support of the Japanese Society for the Promotion of Science (JSPS), Grant No. PE 07021.

[1] V. Burkert and T.-S. H. Lee, Int. J. Mod. Phys. E **13**, 1035 (2004).
[2] A. Matsuyama, T. Sato, and T.-S. H. Lee, Phys. Rep. **439**, 193 (2007), and references therein.
[3] Ch. Sauermann, B. L. Friman, and W. Noerenberg, Phys. Lett. **B341**, 261 (1995).
[4] A. M. Green and S. Wycech, Phys. Rev. C **60**, 035208 (1999).
[5] T. Feuster and U. Mosel, Phys. Rev. C **58**, 457 (1998).
[6] G. Penner, Ph.D. thesis, Universit of Justus-Liebig, Giessen, 2002.
[7] G. Penner and U. Mosel, Phys. Rev. C **66**, 055211 (2002).
[8] A. V. Anisovich, A. V. Sarantsev, O. Bartholomy, E. Klempt, V. A. Nikonov, and U. Thoma, Eur. Phys. J. A **25**, 427 (2005).
[9] A. V. Sarantsev, V. A. Nikonov, A. V. Anisovich, E. Klempt, and U. Thoma, Eur. Phys. J. A **25**, 441 (2005).
[10] M. Batinić, I. Šlaus, A. Švarc, and B. M. K. Nefkens Phys. Rev. C **51**, 2310 (1995); **57**, 1004(E) (1998).
[11] M. Batinić, I. Šlaus, and A. Švarc, Phys. Rev. C **52**, 2188 (1995).
[12] M. Batinić, I. Dadić, I. Šlaus, A. Švarc, B. M. K. Nefkens, and T.-S. H. Lee, arXive: nucl-th/9703023.
[13] S. Ceci, A. Švarc, and B. Zauner, Phys. Rev. Lett. **97**, 062002 (2006).
[14] R. A. Arndt, W. J. Briscoe, I. I. Strakovsky, and R. L. Workman, Phys. Rev. C **74**, 045205 (2006).

[15] T. P. Vrana, Ph.D. thesis, University of Pittsburgh, 1998 (unpublished).
[16] T. P. Vrana, S. A. Dytman, and T.-S. H. Lee, Phys. Rep. **328**, 181 (2000).
[17] B. Juliá-Díaz, T.-S. H. Lee, A. Matsuyama, and T. Sato, Phys. Rev. C **76**, 065201 (2007).
[18] T. Sato and T. S. H. Lee, Phys. Rev. C **54**, 2660 (1996).
[19] G.-Y. Chen, S. Kamalov, S. N. Yang, D. Drechsel, and L. Tiator, Nucl. Phys. **A723**, 447 (2003).
[20] G.-Y. Chen, S. S. Kamalov, S. N. Yang, D. Drechsel, and L. Tiator, Phys. Rev. C **76**, 035206 (2007).
[21] A. M. Gasparyan, J. Haidenbauer, C. Hanhart, and J. Speth, Phys. Rev. C **68**, 045207 (2003).
[22] S. Capstick, T.-S. H. Lee, W. Roberts, and A. Švarc, Phys. Rev. C **59**, R3002 (1999).
[23] X. H. Zhong, Q. Zhao, J. He, and B. Saghai, Phys. Rev. C **76**, 065205 (2007).
[24] B. Saghai, J.-C. David, B. Juliá-Díaz, and T.-S. H. Lee, Eur. Phys. J. A **31**, 512 (2007).
[25] W.-T. Chiang, F. Tabakin, T.-S. H. Lee, and B. Saghai, Phys. Lett. **B517**, 101 (2001).
[26] W.-T. Chiang, B. Saghai, F. Tabakin, and T.-S. H. Lee, Phys. Rev. C **69**, 065208 (2004).
[27] B. Juliá-Díaz, B. Saghai, T.-S. H. Lee, and F. Tabakin, Phys. Rev. C **73**, 055204 (2006).
[28] S. Capstick and W. Roberts, Prog. Part. Nucl. Phys. **45**, 5241 (2000), and references therein.
[29] T. W. Morrison, Ph.D. thesis, George Washington University, UMI-99-55477, 2000.
[30] S. Prakhov *et al*., Phys. Rev. C **72**, 015203 (2005).
[31] W. Deinet *et al*., Nucl. Phys. **B11**, 495 (1969).
[32] W. B. Richards *et al*., Phys. Rev. D **1**, 10 (1970).
[33] N. C. Debenham *et al*., Phys. Rev. D **12**, 2545 (1975).
[34] R. M. Brown *et al*., Nucl. Phys. **B153**, 89 (1979).
[35] H. R. Crouch *et al*., Phys. Rev. D **21**, 3023 (1980).
[36] J. Feltesse *et al*., Nucl. Phys. **B93**, 242 (1975).
[37] V. Z. Peterson *et al*., University of California Radiation Laboratory Report No. UCRL-11576, 1964; F. Bulos *et al*., Phys. Rev. **187**, 1827 (1969); J. E. Nelson, Ph.D. thesis, Lawrence Berkeley Laboratory Report No. LBL-1019, 1972; R. B. Chaffee, Ph.D. thesis, Lawrence Berkeley Laboratory Report No. LBL-1060, 1975.
[38] M. Clajus and B. M. K. Nefkens, $\pi N$ Newslett. **7**, 76 (1992).
[39] H. Kamano, B. Juliá-Díaz, T.-S. H. Lee, A. Matsuyama, and T. Sato, arXiv: 0807.2273 [nucl-th].
[40] W. M. Yao *et al*., J. Phys. G **33**, 1 (2006).
[41] CNS Data Analysis Center, GWU, http://gwdac.phys.gwu.edu.
[42] R. A. Arndt, I. I. Strakovsky, and R. L. Workman, Phys. Rev. C **53**, 430 (1996); Int. J. Mod. Phys. A **18**, 449 (2003).
[43] A. Sibirtsev, S. Schneider, Ch. Elster, J. Haidenbauer, S. Krewald, and J. Speth, Phys. Rev. C **65**, 044007 (2002).
[44] A. M. Green and S. Wycech, Phys. Rev. C **71**, 014001 (2005).
[45] R. A. Arndt, W. J. Briscoe, T. W. Morrison, I. I. Strakovsky, R. L. Workman, and A. B. Gridnev, Phys. Rev. C **72**, 045202 (2005).
[46] J. Caro Ramon, N. Kaiser, S. Wetzel, and W. Weise, Nucl. Phys. **A672**, 249 (2000).
[47] R. S. Bhalerao and L. C. Liu, Phys. Rev. Lett. **54**, 865 (1985); Q. Haider and L. C. Liu, Phys. Lett. **B172**, 257 (1986); C. Bennhold and H. Tanabe, Nucl. Phys. **A530**, 625 (1991).
[48] V. Yu. Grishina, L. A. Kondratyk, M. Buscher, C. Hanhart, J. Haidenbauer, and J. Speth, Phys. Lett. **B475**, 9 (2000).
[49] N. Kaiser, T. Waas, and W. Weise, Nucl. Phys. **A612**, 297 (1997).
[50] Y.-R. Liu and S.-L. Zhu, Phys. Rev. C **75**, 034003 (2007).
[51] T. Inoue, E. Oset, and M. J. Vicente Vacas, Phys. Rev. C **65**, 035204 (2002).
[52] M. Arima, K. Shimizu, and K. Yazaki, Nucl. Phys. **A543**, 613 (1992); V. V. Abaev and B. M. K. Nefkens, Phys. Rev. C **53**, 385 (1996); M. Batinic, I. Slaus, A. Švarc, B. M. K. Nefkens, and T.-S. H. Lee, Phys. Scr. **58**, 15 (1998); O. Krehl, C. Hanhart, C. Krewald, and J. Speth, Phys. Rev. C **62**, 025207 (2000).
[53] Ch. Deutsch-Sauermann, B. L. Friman, and W. Nörenberg, Phys. Lett. **B409**, 51 (1997); A. M. Green and S. Wycech, Phys. Rev. C **55**, R2167 (1997); **60**, 035208 (1999).
[54] H. Calen *et al*., Phys. Rev. Lett. **79**, 2642 (1997); **80**, 2069 (1998).
[55] H. Garcilazo and M. T. Peña, Phys. Rev. C **66**, 034606 (2002).
[56] H. Garcilazo and M. T. Peña, Phys. Rev. C **72**, 014003 (2005).
[57] V. Baru, A. M. Gasparyan, J. Haidenbauer, C. Hanhart, A. E. Kudryavtsev, and J. Speth, Phys. Rev. C **67**, 024002 (2003).
[58] P. Moskal *et al*., Phys. Rev. C **69**, 025203 (2004), and references therein.
[59] R. Shyam, Phys. Rev. C **75**, 055201 (2007).
[60] H.-H. Adam *et al*., Phys. Rev. C **75**, 014004 (2007); J. Smyrski *et al*., Phys. Lett. **B649**, 258 (2007); N. J. Upadhyay, K. P. Khemchandani, B. K. Jain, and N. G. Kelkar, Phys. Rev. C **75**, 054002 (2007); K. P. Khemchandani, N. G. Kelkar, and B. K. Jain, *ibid*. **76**, 069801 (2007).
[61] M. L. Benabderrahmane (FOPI Collaboration), Acta Phys. Polon. B **37**, 167 (2006).
[62] I. G. Alekseev *et al*. (EPECUR and ITEP-PNPI Collaborations), arXiv: hep-ex/0509032.
[63] R. Raja, Nucl. Phys. Proc. Suppl. **175–176**, 17 (2008).
[64] See, for example, J. Imazato, Nucl. Phys. Proc. Suppl. **129**, 81 (2004).
[65] B. Saghai and Z. Li, Eur. Phys. J. A **11**, 217 (2001); J. He, B. Saghai, Z. Li, Q. Zhao, and J. Durand, *ibid*. **35**, 321 (2008); J. He, B. Saghai, and Z. Li, arXiv: 0802.3816 [nucl-th].